Synthesis and Characterization of Alkanethiolate-Coordinated Iron Porphyrins and Their Dioxygen Adducts as Models for the Active Center of Cytochrome P450: Direct Evidence for Hydrogen Bonding to Bound Dioxygen

Fumito Tani,[1a] Mikiya Matsu-ura,[1a] Shinya Nakayama,[1a] Mari Ichimura,[1b] Nobuhumi Nakamura,[1a] and Yoshinori Naruta*,[1a]

Contribution from the Institute for Fundamental Research of Organic Chemistry, Kyushu University, Higashi-ku, Fukuoka 812-8581, Japan, and Department of Chemistry, Graduate School of Science, Kyoto University, Sakyo-ku, Kyoto 606-8502, Japan

Received September 19, 2000

Abstract: Two kinds of novel cytochrome P450 models, which have alkanethiolate axial ligands and hydroxyl groups inside molecular cavities, were designed and synthesized as functional O_2 binding systems. A superstructured porphyrin, designated as "twin-coronet" porphyrin, was used as the common framework of the model complexes. This porphyrin bears four binaphthalene bridges on the both sides and forms two pockets surrounded by the bulky aromatic rings. Thiobenzyloxy and thioglycolate moieties, which contain an alkanethiolate group exhibiting various electron-donating abilities and degrees of bulkiness, were covalently linked to twin-coronet porphyrin to yield thiolate-coordinated hemes, **TCP-TB** and **TCP-TG** (twin-coronet porphyrin with thiobenzyloxy and thioglycolate groups), respectively. Both ferric complexes exhibited high stability during usual experimental manipulation under air and were characterized by MS, UV/vis, ESR spectroscopies, and CV. The ESR spectra exhibited low-spin signals (**TCP-TB**: $g = 2.334, 2.210, 1.959$; **TCP-TG**: $g = 2.313, 2.209, 1.966$). The cyclic voltammogram of **TCP-TB** in CH_3CN gave a quasi-reversible wave which corresponds to the Fe^{III}/Fe^{II} redox couple: $E_{p/2} = -1.35$ V (vs Fc/Fc^+). On the other hand, **TCP-TG** showed a fine reversible wave: $E_{1/2}$ (Fe^{III}/Fe^{II}) $= -1.12$ V. The stable dioxygen adducts were formed in the reaction of the ferric complexes with KO_2 under an oxygen atmosphere and characterized by UV/vis and resonance Raman (RR) spectroscopies. In the RR spectra, the ν(O−O) bands of the dioxygen adducts were observed at 1138 cm^{-1} (**TCP-TB**) and 1137 cm^{-1} (**TCP-TG**). The hypothesis that hydrogen bonding between the bound oxygen and the hydroxyl groups of the binaphthyl moieties could increase their stability was verified by RR spectroscopy. When all hydroxyl groups were deuterated, only the frequencies of the ν(O−O) bands were upshifted by 2 cm^{-1} without any perturbation in the porphyrin skeleton. This work shows the first direct evidence for a hydrogen bond to dioxygen in an oxy form of a thiolate-coordinated heme model system. These results are discussed in context of the process of dioxygen binding and activation in cytochrome P450.

Introduction

A limited number of chemical methodologies[2] have been reported for well-controlled oxygenation of organic substrates by dioxygen with concomitant consumption of a stoichiometric amount of a sacrificial substrate. On the other hand, cytochrome P450 isozymes readily utilize dioxygen to catalyze oxygenation in various biosyntheses of endogenous organic compounds and in detoxification of exogenous ones, generally with high efficiency and selectivity.[3] Gaining an understanding of the oxygenation reaction mechanism of cytochrome P450 could contribute to the design of new oxidation catalysts. Cytochrome P450 as a hemoprotein is structurally distinguished from the large majority of hemoproteins by the presence of a unique thiolate group as an axial ligand to the heme.[4] The strong electron-donor character of the cysteinyl thiolate group to the heme in P450 causes distinct spectroscopic signatures as well as being implicated as a critical structural factor influencing P450's unique reactivity. Both of these distinctive functional and structural features of cytochrome P450 have prompted chemists to prepare synthetic model systems[5] in addition to studying the enzyme itself.

In most reactions mediated by cytochrome P450's, one oxygen atom of a heme-bound dioxygen molecule is inserted into a substrate via heterolysis of the O−O bond, with the other

(1) (a) Kyushu University. (b) Kyoto University.

(2) (a) Mukaiyama, T.; Yamada, T. *Bull. Chem. Soc. Jpn.* **1995**, *68*, 17. (b) Naota, T.; Takaya, H.; Murahashi, S.-I. *Chem. Rev.* **1998**, *98*, 2599.

(3) (a) Ortiz de Montellano, P., Ed. *Cytochrome P-450. Structure, Mechanism, and Biochemistry*, 2nd ed.; Plenum Press: New York, 1995. (b) Watanabe, Y.; Groves, J. T. In *The Enzymes*; Sigman, D. S., Ed.; Academic Press: San Diego, 1992; Vol. 20, p 405.

(4) Poulos, T. L.; Finzel, B. C.; Gunsalus, I. C.; Wagner, G. C.; Kraut, J. *J. Biol. Chem.* **1985**, *260*, 16122.

(5) For typical examples, (a) Ogoshi, H.; Sugimoto, H.; Yoshida, Z. *Tetrahedron Lett.* **1975**, *27*, 2289. (b) Collman, J. P.; E. Groh, S. *J. Am. Chem. Soc.* **1982**, *104*, 1391. (c) Patzelt, H.; Woggon, W. D. *Helv. Chim. Acta* **1992**, *75*, 523. (d) Higuchi, T.; Uzu, S.; Hirobe, M. *J. Am. Chem. Soc.* **1990**, *112*, 7051. (e) Ueyama, N.; Nishikawa, N.; Yamada, Y.; Okamura, T.; Nakamura, A. *J. Am. Chem. Soc.* **1996**, *118*, 12826. (f) Volz, H.; Holtzbecher, M. *Angew. Chem., Int. Ed. Engl.* **1997**, *36*, 1442. (g) Wagenknecht, H. A.; Woggon, W. D. *Angew. Chem., Int. Ed. Engl.* **1997**, *36*, 390. (h) Aissaoui, H.; Bachmann, R.; Schweiger, A.; Woggon, W. D. *Angew. Chem., Int. Ed.* **1998**, *37*, 7, 2998. (i) Tang, S. C.; Koch, S.; Papaefthymiou, G. C.; Foner, S.; Frankel, R. B.; Ibers, J. A.; Holm, R. H. *J. Am. Chem. Soc.* **1976**, *98*, 2414.

10.1021/ja003430y CCC: $20.00
Published on Web 01/18/2001

oxygen atom being reduced to water with two electrons and two protons.[6] Reductive activation of dioxygen by cytochrome $P450_{cam}$, the most thoroughly studied P450, has been postulated to be assisted not only by the heme itself but also by the peripheral amino acids such as Cys-357 and Thr-252, etc., which are conserved in practically all P450 isozymes and are considered to be essential for enzymatic oxygen activation. The thiolate group of Cys-357 axially coordinates to the central iron atom to provide a strong electron donor that increases the electron density of the terminal oxygen atom of the bound dioxygen. The hydroxyl group of Thr-252 and a number of water molecules form a hydrogen-bonding network to relay protons to the terminal oxygen atom.[7,8] The cooperative functions (push−pull effect)[9] of these amino acids could enhance the heterolysis of the dioxygen, and discourage homolysis, so that an active oxidizing species is generated efficiently. However, the entire molecular mechanism of the catalytic cycle, especially the activation of dioxygen, has not yet been fully verified because all of the crucial intermediates have not yet been identified. The dioxygen adduct of P450 is the final intermediate to be observed directly in the catalytic oxygen activation process so far. Preparation of an analogous adduct has been pursued in model studies. However, only a limited number of examples of dioxygen adducts of thiolate-coordinated hemes have been reported[10] due to their characteristic instability. In contrast, there are numerous oxy heme model systems with a nitrogen axial ligand which have been prepared as globin models.[11] The most well-known adducts[10a] utilized extremely electron-deficient arenethiolates as the fifth axial ligand in order to prevent ligand oxidation, instead of an electron-rich alkanethiolate as in the enzyme. To realize the formation of a stable oxygen adduct and to simulate the push−pull effect on the O−O heterolysis, the requisites for the design of a more advanced model are the following: (1) A hydrophobic pocket for oxygen binding to iron, (2) axial coordination of a well-sheltered alkanethiolate anion for the strong electron demand at the stage of O−O bond cleavage, and (3) hydrogen bonding to the bound dioxygen for the stabilization of the adduct and for proton donation. A hydrogen bond to the bound dioxygen has never been observed for previous models for P450. Thus, we designed and prepared two kinds of alkanethiolate-coordinated model hemes,[12] that fulfill the above requirements. The stable dioxygen adducts were prepared from the ferric complexes and characterized by UV/vis and resonance Raman (RR) spectroscopies. In addition, direct evidence for hydrogen bonding to the bound dioxygen was obtained. These complexes increase our understanding of the mechanism of dioxygen activation by cytochrome P450.

Results and Discussion

Design and Synthesis of P450 Models. The following are the most important features of our design of **TCP-TB** and **TCP-TG** (twin coronet porphyrins[13] with thiobenzyloxy and thioglycolate groups): (1) On both sides of the porphyrin plane, bulky binaphthyl moieties can form hydrophobic molecular cavities, which are suitable for the creation of an oxygen binding site to prevent irreversible autoxidation of the iron center. (2) In one of the cavities, an alkanethiolate group is covalently fixed to coordinate axially to the central iron and is sterically protected from undesirable disulfide formation and other oxidative decomposition. (3) In the opposite cavity, two naphtholic hydroxyl groups are oriented toward the center above the heme with the objective of forming a hydrogen bond to bound dioxygen. (4) To prepare hemes having an alkanethiolate ligand of different steric and electronic character, two kinds of alkanethiolates were chosen. The thiolate moiety of **TCP-TG** is more compact and less electron-donating due to its ester-carbonyl group than that of **TCP-TB**.

First, the major framework, twin-coronet porphyrin (**TCP**), is synthesized by making bridges between the *ortho* positions of the adjacent *meso* aryl rings with binaphthyl derivatives through ethereal linkages (Scheme 1). Next, a protected thiolate moiety is covalently fixed into one of the cavities. Finally, metal insertion and the deprotection of the thiolate group are accomplished. Hence, *meso*-tetrakis(2,6-dihydroxylphenyl)porphine **1**, optically active binaphthyl derivative **5**, and protected-thiolate derivatives **7** or **8** are necessary.

The porphyrin **1** was obtained from *meso*-tetrakis(2,6-dimethoxyphenyl)porphine, which was synthesized by clay-mediated condensation[14] between 2,6-dimethoxybenzaldehyde and pyrrole. Montmorillonite K10 clay functions as an acid catalyst and an efficient template for macrocycle formation from linear pyrrole oligomers. In terms of simplicity and yield, the procedures using K10 are superior to previous ones[13a,15] which utilized Adler[16] or Lindsey[17] methods. The demethylation reaction was carried out with pyridinium hydrochloride to give **1** in a satisfactory yield.

To avoid formation of many isomers in the reaction of **1** and **5**, optically pure (*S*)-1,1′-bi-2-naphthol was used as a starting compound for the synthesis of **5** (Scheme 2). On the basis of the following requirements, the methoxymethyl (MOM) group was chosen for the protection of the hydroxyl groups. (1) It should be stable during the condensation reaction under basic and high-temperature conditions. (2) It should be compact enough to avoid possible steric repulsion between the porphyrin and the binaphthyl derivatives. (3) It should be selectively removable under mild conditions, because similar ether groups, phenyl benzyl ether, exist in **TCP 9a**.

Even very careful *ortho* lithiation and formylation of **2** gave unavoidably a mixture of dialdehyde **3** and monoaldehyde as a

(6) (a) Sono, M.; Roach, M. P.; Coulter, E. D.; Dawson, J. H. *Chem. Rev.* **1996**, *96*, 2841. (b) Shimada, H.; Sligar, S. G.; Xeom, H.; Ishimura, Y. In *Oxygenase and Model Systems*; Funabiki, F., Ed.; Kluwer Academic: Dordrechet, 1997; p 195.

(7) (a) Imai, M.; Shimada, H.; Watanabe, Y.; Matsushima-Hibiya, Y.; Makino, R.; Koga, H.; Horiguchi, T.; Ishimura, Y. *Proc. Natl. Acad. Sci. U.S.A.* **1989**, *86*, 7823. (b) Gerber, N. C.; Sligar, S. G. *J. Am. Chem. Soc.* **1992**, *114*, 8742. (c) Vidakovic, M.; Sligar, S. G.; Li, H.; Poulos, T. L. *Biochemistry* **1998**, *37*, 9211.

(8) Schlichting, I.; Berendzen, J.; Chu, K.; Stock, A. M.; Maves, S. A.; Benson, D. E.; Seet, R. M.; Ringe, D.; Petsko, G. A.; Sligar, S. G. *Science* **2000**, *287*, 1615.

(9) (a) Dawson, J. H. *Science* **1988**, *240*, 433. (b) Poulos, T. L. *Adv. Inorg. Biochem.* **1988**, *7*, 1.

(10) (a) Schappacher, M.; Ricard, L.; Fisher, J.; Weiss, R.; Bill, E.; Montiel-Montoya, R.; Winkler, H.; Trautwein, A. X. *Eur. J. Biochem.* **1987**, *168*, 419. (b) Kasmi, D. EI.; Tetreau, C.; Lavatte, D.; Momenteau, M. *J. Am. Chem. Soc.* **1995**, *117*, 6041.

(11) Momenteau, M.; Reed, C. A. *Chem. Rev.* **1994**, *94*, 659 and references therein.

(12) For our preliminary reports, see: (a) Tani, F.; Nakayama, S.; Ichimura, M.; Nakamura, N.; Naruta, Y. *Chem. Lett.* **1999**, 729. (b) Matsuura, M.; Tani, F.; Nakayama, S.; Nakamura, N.; Naruta, Y. *Angew. Chem., Int. Ed.* **2000**, *39*, 1989.

(13) We already reported that similar **TCP** complexes catalyzed asymmetric oxidation of olefins and sulfides with high enantio selectivity: (a) Naruta, Y.; Tani, F.; Ishihara, N.; Maruyama, K. *J. Am. Chem. Soc.* **1991**, *113*, 6865. (b) Naruta, Y.; Tani, F.; Maruyama, K. *Tetrahedron: Asymmetry* **1991**, *2*, 533.

(14) Onaka, M.; Shinoda, T.; Izumi, Y.; Nolen, E. *Tetrahedron Lett.* **1993**, *34*, 2625.

(15) (a) Tsuchida, E.; Hasegawa, E.; Komatsu, T.; Nakata, T.; Nagano, K.; Nishida, H. *Bull. Chem. Soc. Jpn.* **1991**, *64*, 888. (b) Collman, J. P.; Lee, V. J.; Zhang, X. *Inorg. Synth.* **1996**, *31*, 117.

(16) Adler, A. D. *J. Org. Chem.* **1967**, *32*, 476.

(17) Lindsey, J. S.; Wagner, R. W. *J. Org. Chem.* **1989**, *54*, 828.

Scheme 1[a]

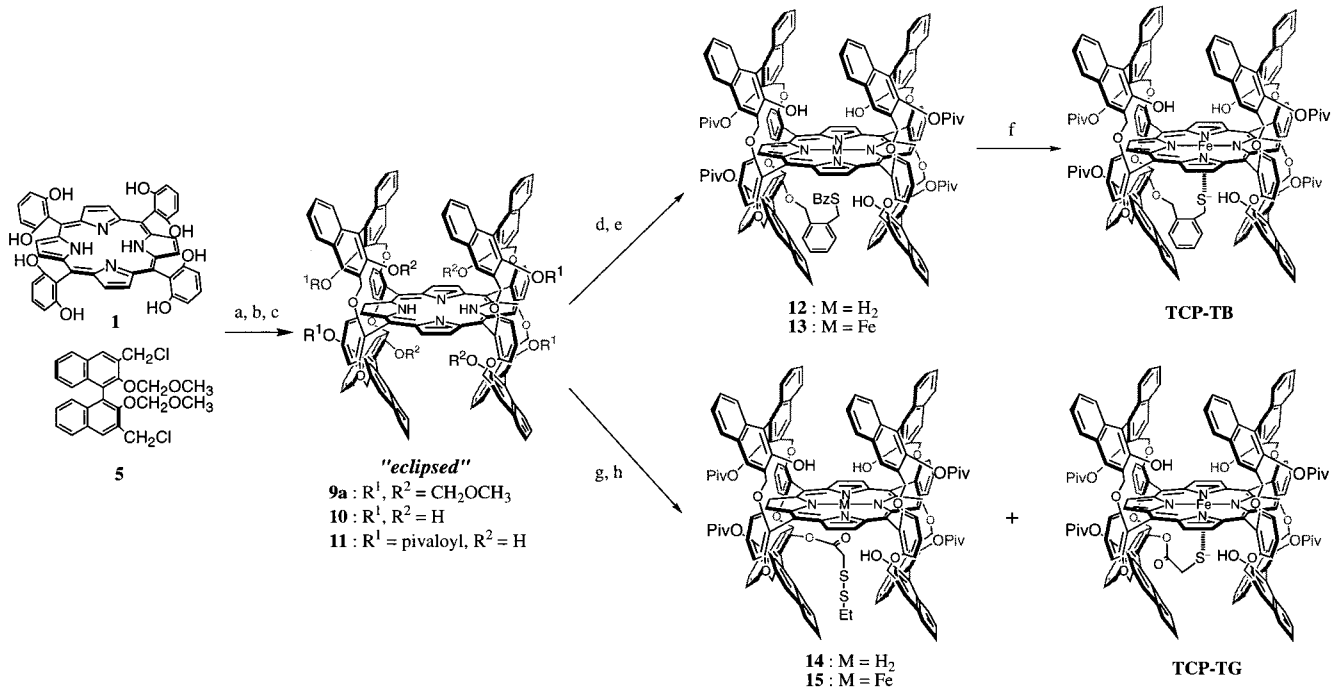

[a] Reagents and conditions: (a) K_2CO_3, THF, NMP, 110 °C, 19%. (b) trimethylsilyl bromide, CH_2Cl_2, −40 °C, 96%. (c) pivaloyl chloride, pyridine, CH_2Cl_2, 97%. (d) **7**, K_2CO_3, NMP, 100 °C, 62%. (e) $Fe(CO)_5$, I_2, toluene, 50 °C, 78%. (f) $BuNH_2$, CH_3CN, 48%. (g) **8**, 1-(3-dimethylaminopropyl)-3-ethylcarbodiimide hydrochloride, 4-(dimethylamino)pyridine, CH_2Cl_2, 36%. (h) $Fe(CO)_5$, I_2, toluene, 50 °C, 41% (**TCP-TG**), 16% (**15**).

Scheme 2

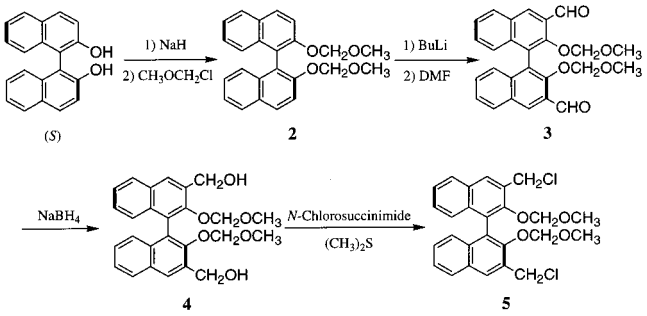

minor product. Fortunately, **3** was purified by recrystallization from ether to give fine, pale-yellow crystals.[18] Reduction of **3** and subsequent chlorination of **4** with NCS under neutral conditions[19] afforded the corresponding dichloride **5** in a good yield.

According to the procedure of the previous report[13a] with some improvements, the major framework of the binaphthalene-bridged **TCP** was prepared by the condensation of the octahydroxylated TPP **1** and the binaphthyl dichloride **5** under basic conditions (Scheme 1). A THF−NMP solution of **1** and **5** was heated at 115−120 °C with K_2CO_3 under a high-purity nitrogen atmosphere. The resultant two isomers were separated carefully by column chromatography and distinguished by characteristic ^{1}H NMR signals of the pyrrole β-protons (Table 1). The less polar isomer showed signals of the β-protons as a pair of singlets, while two doublet peaks appeared in the case of the more polar isomer. On the basis of their spectroscopic features, the less polar isomer and the more polar one were assigned to be eclipsed **9a** and staggered **9b**,[20] respectively. Only the eclipsed isomer **9a** was further used in the following reactions. The MOM-protecting groups were removed with trimethylsilyl bromide[21] in an excellent yield (96%), which more than doubled the previous yield of ca. 45% observed when pyridinium *p*-toluenesulfonate (PPTS) was used as a deprotecting reagent. Deprotection by PPTS[22] resulted in the formation of various byproducts and a low yield with poor reproducibility. The selective reprotection of the outer four hydroxyl groups of **10** was accomplished with bulky pivaloyl chloride, while the inner four hydroxyl groups remained free. Since these porphyrin molecules **9**−**11** have high symmetry (D_2); the four binaphthalene moieties of each compound are equivalent. The ^{1}H NMR spectra of **9**−**11** showed simpler patterns than those of porphyrins **12** and **14,** which have no symmetry due to their protected-thiolate group substituents.

Table 1. ^{1}H NMR Chemical Shifts of Selected Protons of Twin-Coronet Porphyrins[a]

compound	pyrrole β-H	piv-CH_3	NH
9a	8.69, 8.50 (each s)	-	−2.42
9b	8.67, 8.49 (each d)	-	−2.99
10	8.74, 8.54 (each s)	-	−2.81
11	8.77, 8.41 (each s)	0.51	−3.01
12	8.73, 8.70, 8.58, 8.57	0.77, 0.74	−3.62
	8.54, 8.50, 8.16, 8.11	0.28, 0.17	
	(each d)		
14	8.82, 8.79, 8.77, 8.76	0.73, 0.68	−2.94
	8.62, 8.55, 8.30, 8.27	0.33, 0.23	
	(each d)		

[a] The detailed ^{1}H NMR data of **9a**−**11** are included in Supporting Information.

(18) The three-dimensional structure of **3** was revealed by X-ray crystallographic analysis. Tachi, Y.; Nakayama, S.; Tani, F.; Ueno, G.; Naruta, Y. *Acta Crystallogr.* **1999**, *C55*, 1351.

(19) Since MOM-protecting group is labile under acidic conditions, conventional chlorinating reagents, such as $SOCl_2$ and PCl_3, cannot be used. Corey, E. J.; Kim, C. U.; Takeda, M. *Tetrahedron Lett.* **1972**, *13*, 4339.

(20) The staggered isomer **9b** is omitted in Scheme 1. In **9b**, the positions of the binaphthalene bridges are different between the upper and lower sides of the porphyrin plane. See ref 13a.

(21) Hanessian, S.; Delorme, D.; Dufresne, Y. *Tetrahedron Lett.* **1984**, *25*, 2515.

(22) Monti, H.; Leandri, G.; Klos-Ringquet, M.; Corriol, C. *Synth. Commun.* **1983**, *13*, 1021.

Scheme 3

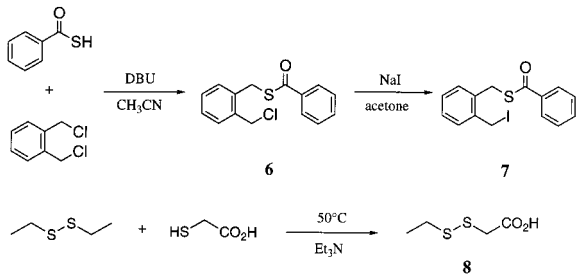

The thiolate moiety was designed with the following considerations: (1) It should contain another functional group, which can be linked to one of the inner hydroxyl groups. (2) It should not be too large to fit inside the sterically hindered cavity. (3) The sulfur atom should favorably coordinate to the iron. (4) The protecting group of the thiolate should be intact at the stage of the condensation reaction and should be selectively removable at the final stage under mild conditions, keeping the other potentially labile groups undamaged, such as the resulting thiolate group, the *O*-pivaloyl ester, and the linkage between the thiolate moiety and the porphyrin. The syntheses of two different protected thiolate derivatives, **7** and **8**, which satisfy the above requirements, were carried out as follows (Scheme 3). The reaction of thiobenzoic acid with 1,2-bis(chloromethyl)-benzene was accomplished under basic conditions[23] to give 2-(chloromethyl)benzyl thiobenzoate **6**. Two electrophilic carbon atoms in **6**, the chloro-substituted carbon and the thioester carbonyl carbon, are potentially reactive to the nucleophilic naphtholate anion.[24] To enhance the reactivity of the halogen-substituted carbon, **6** was converted to the corresponding iodide **7** via a halogen-exchange reaction. Ethyldisulfanylacetic acid, **8**, was obtained by the reaction of thioglycolic acid and ethyl disulfide at 50 °C.[25] Disulfide protection can be cleaved by reductive halogenation with I_2 as a mild nucleophile.[26] The use of $Fe(CO)_5$ and I_2 in the final step of the synthesis of **TCP-TG** allows iron insertion and the deprotection to be accomplished simply and efficiently in one pot.

The coupling reaction between porphyrin **11** and 2-(iodomethyl)benzyl thiobenzoate,**7**, in the presence of K_2CO_3 gave the desired **12**, where the protected thiolate moiety is connected through an ether linkage. The ^{1}H NMR spectrum of **12** shows fairly complicated patterns; the eight pyrrole β-protons appear separately as eight doublets, and the four pivaloyl groups show four distinct singlets. This indicates complete loss of the symmetry in **12**. The free base porphyrin **12** was converted to the corresponding ferric complex **13** with $Fe(CO)_5$ and I_2. Nucleophilic attack of a primary amine to the carboxyl carbon of a *S*-ester is favored over that of an *O*-ester, resulting in the corresponding thiol and amide.[27] On the basis of this knowledge, the selective deprotection of the thioester group in **13** was achieved with $BuNH_2$, without any cleavage of the pivaloyl ester groups, to afford the thiolate-coordinated ferric complex **TCP-TB**. This compound was stable enough to allow purification by column chromatography on silica gel under air.

(23) (a) Ono, N.; Yamada, T.; Saito, T.; Tanaka, K.; Kaji, A. *Bull. Chem. Soc. Jpn.* **1978**, *51*, 2401. (b) Rao, C. G. *Org. Prep. Proced. Int.* **1980**, *12*, 225.

(24) In fact, the use of the chloride **6** led only to the formation of the corresponding benzoyl ester of the naphthol group through ester exchange reaction instead of *O*-alkylation.

(25) Armitage, D. A.; Clark, M. J.; Tso, C. C. *J. Chem. Soc., Perkin Trans. I* **1972**, 681.

(26) Pryor, W. A. *Mechanisms of Sulfur Reactions*; McGraw-Hill: New York, 1962; p 60.

(27) Fuchs, G. *Acta Chem. Scand.* **1965**, *19*, 1490.

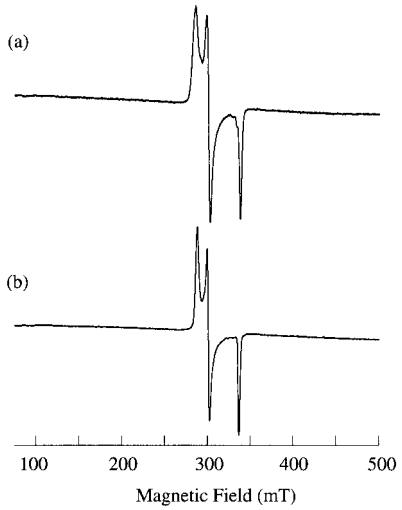

Figure 1. ESR spectra of (a) **TCP-TB** and (b) **TCP-TG** in THF at 77 K. Microwave frequency (a) 9.24924 GHz, (b) 9.24946 GHz, power 1 mW, modulation amplitude 1 mT, modulation frequency 100 kHz.

For the preparation of **TCP-TG**, ethyldisulfanylacetic acid, **8**, was connected to one of the inner hydroxyl groups of **11** through an ester linkage. The resultant coupling product **14** also shows a ^{1}H NMR spectrum as complicated as that of **12**. Chemical shifts of the thiolate moiety, which was strongly shielded by the porphyrin ring current, are significantly shifted to upper field. Chemical shifts for the ethyl group are $\delta = -0.44, -1.20$ and for the methylene group are $\delta = -2.15, -2.72$. It is noteworthy that, at the final step in this synthesis, the iron insertion and the deprotection of the thiolate group were simultaneously achieved to yield the thiolate-coordinated ferric heme **TCP-TG** with concomitant production of the thiolate-protected iron complex **15**. When the same reaction was carried out at ambient temperature, **15** was obtained as a major product. Both of these complexes exhibited sufficient stability for usual manipulation under aerobic conditions. Compared to the thiolate-protected ferric complexes, **13** and **15**, **TCP-TB** and **TCP-TG** were less polar on silica gel TLC and were easily purified by column chromatography. Generally, a ferric heme having no anionic group bears a counteranion and consequently shows high polarity. On the other hand, a thiolate-coordinated ferric heme is a neutral molecule due to the negative charge of the intramolecularly coordinated thiolate anion. This characteristic TLC behavior provides a convenient probe for the screening thiolate-coordinated ferric heme complexes.

Spectroscopic Characterization of the Thiolate-Ligated Model Complexes. ESI-MS spectra of the thiolate-ligated model complexes showed molecular ion peaks at $m/z = 2509.8$ (**TCP-TB**) and 2447.0 (**TCP-TG**), respectively. The isotopic patterns were in good accordance with their simulation. Moreover, the observed mass numbers in high-resolution FAB-MS were also in good agreement with the calculated mass numbers. These experimental data indicate the successful preparation of the desired complexes. Electronic spectra of ferric **TCP-TB** and **TCP-TG** in CH_2Cl_2 were essentially identical, exhibiting Soret bands at $\lambda_{max} = 416-418$ nm and visible bands at $\lambda_{max} = 513-515$ nm. The thiolate-protected ferric complexes, **13** and **15**, showed Soret bands at $\lambda_{max} = 421-423$ nm, which are slightly red-shifted compared to those of the thiolate-ligated complexes.

ESR spectra of **TCP-TB** and **TCP-TG** were measured in THF at 77 K (Figure 1 and Table 2). The ESR spectra of these complexes clearly showed near-axial rhombic low-spin signals. The two crystal field parameters, tetragonality $|\mu/\lambda|$ and rhom-

Scheme 4

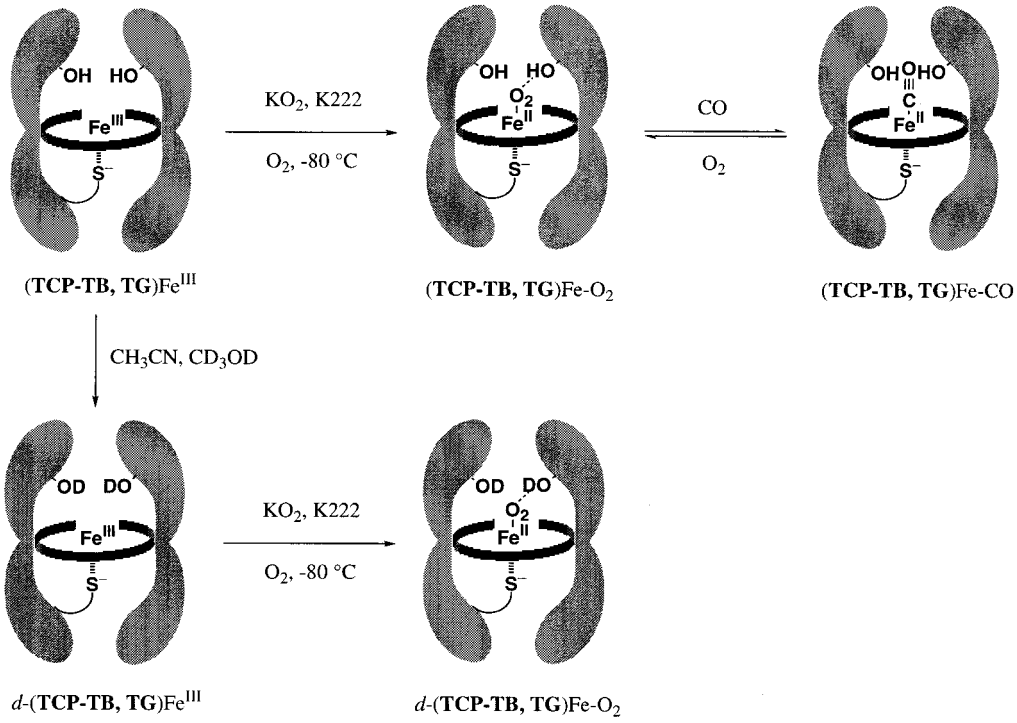

Table 2. ESR Spectroscopic Data of Thiolate-Ligated Hemes

	ESR *g* value			crystal field parameter	
	g_1	g_2	g_3	$\|\mu/\lambda\|$	$\|R/\mu\|$
TCP-TB	2.334	2.210	1.959	8.230	0.414
TCP-TG	2.313	2.209	1.966	8.512	0.370
$P450_{cam}$[a]	2.45	2.26	1.91	5.998	0.469

[a] Reference 5i.

bicity $|R/\mu|$, both of which are calculated from *g* values, have been used to evaluate rhombic types of low-spin ferric hemoproteins and their model complexes.[28] By Bohan's method,[29] two crystal field parameters, $|\mu/\lambda|$ and $|R/\mu|$, were determined from the three observed *g* values to be 8.230, 0.414 (**TCP-TB**) and 8.512, 0.370 (**TCP-TG**), respectively. According to the classification of axial donor ligands based on the crystal field parameters,[30] these values are included in the range of six-coordinate low-spin ferric hemes with a thiolate axial ligand and an oxygen-donor ligand.[31] Compared with cytochrome $P450_{cam}$, **TCP-TB** and **TCP-TG** showed higher tetragonality and lower rhombicity values, indicating relatively high axial symmetry and strong electron donation from the thiolate ligands. A previous alkanethiolate-coordinated model complex exhibited very similar ESR features ($g = 2.32, 2.21, 1.96$).[5d]

(28) (a) Griffith, J. S. *Nature* **1957**, *180*, 30. (b) Kotani, M. *Suppl. Prog. Theor. Phys.* **1961**, *17*, 4. (c) Peisach, J.; Blumberg, W. E.; Alder, A. *Ann. N.Y. Acad. Sci.* **1973**, *206*, 310. (d) Blumberg, W. E.; Peisach, J. In *Probes of Structure and Function of Macromolecules and Membranes*; Chance, B., Yonetani, T., Mildoon, A. S., Eds.; Academic: New York, 1971; Vol. II, p 215. (e) Blumberg, W. E.; Peisach, J. In *Bioinorganic Chemistry*; Gould, R. F., Ed.; American Chemical Society: Washington, DC, 1971; p 271.

(29) Bohan, T. L. *J. Magn. Reson.* **1977**, *26*, 109.

(30) Sakurai, H.; Yoshimura, T. *J. Inorg. Biochem* **1985**, *24*, 75.

(31) Under these ESR conditions in THF, the solvent molecule itself was likely to the sixth ligand of **TCP-TB** and **TCP-TG**, based on the experimental results. Their UV/vis spectra in THF were quite different from those in a noncoordinating solvent such as toluene. Nonetheless, addition of even a small amount (2−3% volume) of THF to their toluene solutions turned their spectra identical to those in THF, indicating the axial coordination of THF. The assumption that THF is the sixth ligand is also consistent with the observed ESR parameters. UV/vis; **TCP-TB**, λ_{max} (toluene) 325, 350, 421, 512, 624 nm; **TCP-TG**, λ_{max} (toluene) 325, 340, 418, 511, 575, 649 nm.

Table 3. Reduction Potentials of **TCP-TB**, **TCP-TG**, and FeTMPCl[a]

	reduction potentials/V, Fe(III)/Fe(II)	
complex	vs Fc/Fc^{+c}	vs NHE
TCP-TB; $E_{p/2}$	−1.35	(−0.95)
TCP-TG; $E_{1/2}$	−1.12	(−0.72)
FeTMPCl;[b] $E_{1/2}$	−0.73	(−0.33)
$P450_{cam}$;[d] $E_{1/2}$	-	−0.33

[a] 0.1 M Bu_4NBF_4/CH_3CN with Pt working/counter electrodes, [Fe-por] = 0.5 mM, at scanning rate 50 mV/sec. [b] FeTMPCl= iron *meso*-tetramesityl-porphyrin chloride. [c] Fc = ferrocene. [d] Reference 6a.

The reduction potentials of **TCP-TB** and **TCP-TG** were determined by cyclic voltammetry (Table 3). A quasi-reversible Fe^{III}/Fe^{II} couple was observed in the voltammogram of **TCP-TB**, while **TCP-TG** showed a reversible couple. The slightly positive-shifted potential of **TCP-TG** is ascribed to the coordination of the less electron-donating thiolate ligand relative to that of **TCP-TB**. The potentials versus NHE of **TCP-TB** and **TCP-TG** were estimated to be −0.95 and −0.72 V, respectively, from the observed potentials. This indicates that **TCP-TG** has a potential closer to that of low-spin cytochrome $P450_{cam}$[6a] than **TCP-TB**. The more negative potentials of both **TCP-TB** and **TCP-TG** compared to those of iron *meso*-tetramesitylporphyrin chloride and cytochrome $P450_{cam}$, indicate that strong electron donation occurs mainly from the thiolate ligands to the iron atoms.

Formation and Characterization of Dioxygen Adducts. Valentine and co-workers reported reactions of superoxide anion, O_2^-, with ferric porphyrins and found that two types of reactions occurred which depend on conditions: one-electron reduction of an iron center or formation of a dioxygen adduct.[32] Using their methods, we have obtained dioxygen adducts directly from the ferric forms of **TCP-TB** and **TCP-TG** by addition of an equimolar amount of KO_2 under an oxygen

(32) McCandlish, E.; Miksztal, A. R.; Nappa, M.; Sprenger, A. Q.; Valentine, J. S.; Stong, J. D.; Spiro, T. G. *J. Am. Chem. Soc.* **1980**, *102*, 4268.

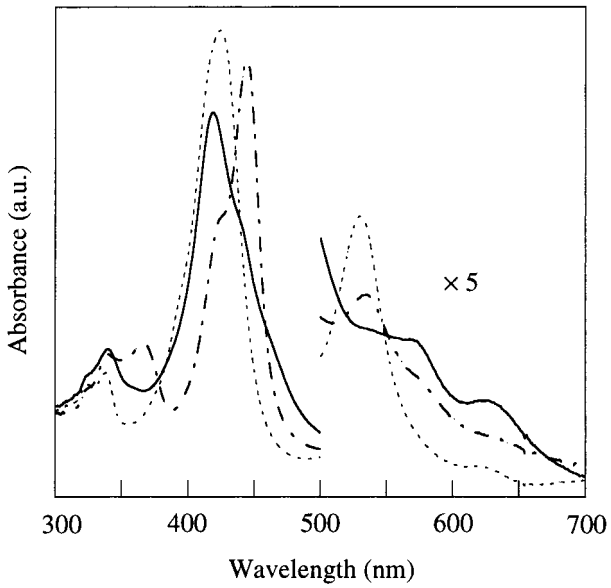

Figure 2. UV/vis spectra of O_2, CO, ferric complexes of **TCP-TG** in THF at −80 °C: full line, O_2 complex; dash−dot line, CO complex; broken line, ferric complex.

Table 4. Electronic Absorption Data for Ferric, CO, and O_2 Complexes[a]

complex	λ_{max}/nm
(**TCP-TB**)Fe^{III}	340, 423, 532
(**TCP-TB**)Fe−CO	342, 360, 445, 529
(**TCP-TB**)Fe−O_2	339, 424, 532, 642
(**TCP-TG**)Fe^{III}	337, 424, 530
(**TCP-TG**)Fe−CO	366, 444, 537
(**TCP-TG**)Fe−O_2	339, 421, 544, 629

[a] In THF, −80 °C.

atmosphere (Scheme 4).[33] Addition of KO_2 to a THF solution of the ferric complex (**TCP-TB**, **TG**)Fe^{III} at −80 °C induced an immediate and drastic change in the UV/vis spectrum (Figure 2 and Table 4). The absorbance of the Soret band slightly decreased, and the intensity of Q-band around 530 nm significantly decreased. When the atmosphere was replaced with CO, the dioxygen adducts were converted to the corresponding CO adducts, which exhibit typical hyperporphyrin spectra with split Soret bands. The reversibility of the O_2/CO exchange indicates that the ferrous oxidation state and the axial coordination of the thiolate remain under these conditions without any autoxidation or other oxidative decomposition. The thermal stability of these dioxygen adducts are fairly high, especially in the case of **TCP-TG**. The UV/vis spectra of the adducts were stable and unchanged at elevated temperatures up to −20 °C for **TCP-TB** ($t_{1/2}$ at −20 °C ≈ 1 h) and 0 °C for **TCP-TG** ($t_{1/2}$ at 0 °C ≈ 5 h). The differences in thermal stability of the two complexes could be due to differences in electron density at the iron, resulting from the strength of the electron donation from the axial thiolate ligand, as already shown in the electrochemical data.

Resonance Raman (RR) spectroscopy is a very powerful technique for elucidating the detailed active-site structures of

(33) A dioxygen adduct of a heme is generally prepared stepwise through reduction of a ferric complex to the ferrous one under aqueous conditions and subsequent addition of dioxygen gas. However, during the reduction of ferric **TCP-TB** and **TCP-TG** under protic conditions, such as with aqueous dithionite solution, the thiolate−ferrous complexes are easily protonated to turn into the thiol-coordinated ones with the neutralization of the unstable negative charge. Therefore, we selected the direct aprotic method by the use of KO_2. See ref 12a.

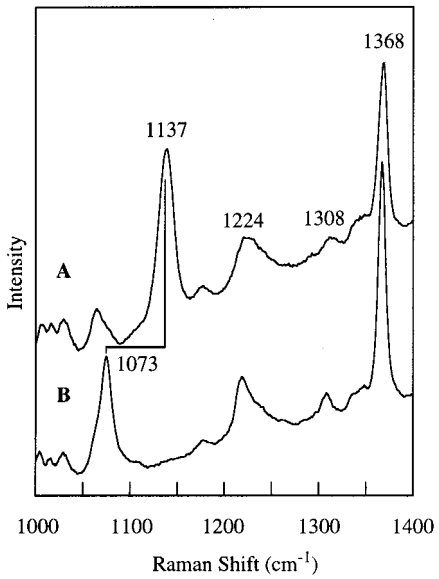

Figure 3. High-frequency region of resonance Raman spectra of the dioxygen adduct of **TCP-TG**. THF/CH_3CN, −60 °C, 413.1 nm excitation, 20 mW: trace **A**, $K^{16}O_2$ + $^{16}O_2$; trace **B**, $K^{18}O_2$ + $^{18}O_2$. The RR spectra of the dioxygen adduct of **TCP-TP** are included in Supporting Information.

Table 5. Summary of ν(O−O) Frequencies for Dioxygen Adducts of Thiolate-Coordinated Hemes

complex	ν(O−O)[a]/cm^{-1}	reference
($P450_{cam}$)Fe−O_2/camphor	1140 (1074)	36, 37
($P450_{cam}$)Fe−O_2/adamantanone	1147 (1080)	36
($C_6HF_4S^-$)($TP_{piv}P$)Fe−O_2	1140 (1080)	36, 38
($C_6F_5S^-$)($TP_{piv}P$)Fe−O_2	1147 (1084)	36
(**TCP-TB**)Fe−O_2	1138 (1074)	this work
(**TCP-TG**)Fe−O_2	1137 (1073)	this work

[a] Values in parentheses are for $^{18}O_2$ adducts.

hemoproteins and their model systems.[34] RR spectra have also been obtained for cytochrome P450 enzymes from various origins.[35] We have applied RR spectroscopy to the dioxygen adducts of **TCP-TB** and **TCP-TG** in order to verify the existence of the Fe−O_2 moiety. The RR spectra of the dioxygen adducts obtained with Soret excitation exhibited a strong line at 1138 cm^{-1} for **TCP-TB** and 1137 cm^{-1} for **TCP-TG** (Figure 3). By replacing $K^{16}O_2$ and $^{16}O_2$ with $K^{18}O_2$ and $^{18}O_2$, these lines shifted to 1074 and 1073 cm^{-1}, respectively. The observed isotopic shifts upon $^{18}O_2$ substitution are in good agreement with the value calculated from the harmonic oscillator approximation of the O−O stretching vibration ($\Delta_{obs}(^{16}O_2/^{18}O_2)$ = 64 cm^{-1}; Δ_{calc} = 65 cm^{-1}). These bands are therefore assigned to the ν(O−O) mode. The ν(O−O) frequencies of oxy thiolate-coordinated hemes determined by RR spectroscopy, are summarized in Table 5. The observed frequencies of the ν(O−O) modes are very close to those of oxy-cytochrome $P450_{cam}$[36,37]

(34) Spiro, T. G. Ed. *Biological Applications of Raman Spectroscopy*; John Wiley: New York, 1988; Vol. 3.

(35) (a) Champion, P. M.; Gunsalus, I. C.; Wagner, G. C. *J. Am. Chem. Soc.* **1978**, *100*, 3743. (b) Ozaki, Y.; Kitagawa, T.; Kyogoku, Y.; Imai, Y.; Hashimoto-Yutsudo, C.; Sato, R. *Biochemistry* **1978**, *17*, 5827. (c) Shimizu, T.; Kitagawa, T.; Mitani, F.; Iizuka, T.; Ishimura, Y. *Biochim. Biophys. Acta* **1981**, *670*, 236.

(36) Hu, S.; Schneider, A. J.; Kincaid, J. R. *J. Am. Chem. Soc.* **1991**, *113*, 4815.

(37) (a) Bangchaoenpaurpong, O.; Rizos, A. K.; Champion, P. M.; Jollie, D.; Sligar, S. *J. Biol. Chem.* **1986**, *261*, 8089. (b) Macdonald, I. D. G.; Sligar, S. G.; Christian, J. F.; Unno, M.; Champion, P. M. *J. Am. Chem. Soc.* **1999**, *121*, 376. (c) Egawa, T.; Ogura, T.; Makino, R.; Ishimura, Y.; Kitagawa, T. *J. Biol. Chem.* **1991**, *266*, 10246.

and oxy-model complexes.[36,38] A Raman active ν(O−O) mode has been found to be characteristic of the dioxygen adduct of a thiolate-coordinated heme. In contrast, the ν(O−O) mode of an oxy heme with an axial ligand of a nitrogen-base is Raman inactive.[39] Simultaneous enhancement of M−O_2 and O−O stretching vibrations was first observed by Yu and co-workers in oxycobalt myoglobin and hemoglobin.[40] They suggested that the enhancement was attributed to the charge-transfer transition from the occupied $\pi^*(p_g^*/d_{xz})$ to empty antibonding $\sigma^*(d_{z^2}/p_g^*)$ orbital. For an oxy iron porphyrin, it is impossible to have charge transfer from π^* to σ^*, since the π^* orbital is no longer populated. However, RR enhancement of ν(Fe−O_2) and ν(O−O) was found in a thiolate-coordinated oxy heme and explained as follows: the thiolate ligand increases the electron density of porphyrin π^* through p_π and d_π to promote the charge-transfer transition from the π^* to the empty Fe−O π^* orbital of the oxy form which then leads to the enhancement of ν(O−O) band. Therefore, the present RR results reveal successful formation of the desired dioxygen adducts of the thiolate-coordinated hemes. However, no oxygen-sensitive bands, corresponding to ν(Fe−O_2) and δ(Fe−O−O), were detectable in the low-frequency region in the RR spectra of both the adducts with Soret excitation (413.1, 441.6 nm)

It is notable that the oxidation marker band (ν_4) of oxy **TCP-TB** and **TCP-TG** appeared at 1368 cm^{-1}. This value is lower by 6 cm^{-1} than that of the oxy-cytochrome $P450_{cam}$.[36] The vibrational modes of porphyrin skeleton are empirically correlated with heme core size and are very useful for determining the spin and oxidation state of the heme iron. The ν_4 band, which can be clearly identified without interference from other modes, is sensitive to the electron population in the π^* antibonding orbitals of the porphyrin ring. When the π^* orbital increases in population, the frequency of ν_4 decreases. Hence, the electron densities of the iron centers of our dioxygen adducts are considered to be higher than that of oxy-cytochrome $P450_{cam}$, as predicted from the electrochemical data.

Evidence for Hydrogen Bonding to Bound Dioxygen. The thermal stability of these dioxygen adducts was also confirmed by RR spectroscopy. The ν(O−O) bands were successfully observed at −20 °C (**TCP-TB**) and 0 °C (**TCP-TG**), respectively. Despite the coordination of the strongly electron-donating alkanethiolate anions, these dioxygen adducts exhibited high thermal stability. We postulated that an intramolecular hydrogen bond between the bound oxygen and the hydroxyl groups of the binaphthalene moieties was mainly responsible for this higher stability. To verify this prediction, we investigated the frequencies of the O−O stretching modes of the dioxygen adduct upon deuterium substitution of the exchangeable protons. After ferric **TCP-TB** and **TCP-TG** were kept in CH_3OH/CH_3CN or CD_3OD/CH_3CN for several hours and dried in vacuo overnight, the reaction with KO_2 was carried out (Scheme 4). In the IR spectra of ferric **TCP-TB** and **TCP-TG**, ν(O−H) signals (**TCP-TB**: 3489, 3443 cm^{-1}, **TCP-TG**: 3453 cm^{-1}) were replaced with lower ν(O−D) bands (**TCP-TB**: 2588, 2549 cm^{-1}, **TCP-TG**: 2558 cm^{-1}) upon H/D exchange treatment, and no other bands were shifted. In the RR spectra of both oxy-**TCP-TB** and **TCP-TG**, only the ν(O−O) modes were upshifted by 2 cm^{-1} upon exchange of CH_3OH by CD_3OD (Figure 4 and Table 6). No other vibrations exhibited frequency shifts. These results indicate that there is no perturbation in the porphyrin skeleton upon H/D exchange. Using RR spectroscopy, two groups have independently reported the upshifts of ν(O−O) mode of oxycobalt myoglobin and hemoglobin on replacement of H_2O with D_2O.[41] However, their interpretations of the ν(O−O) mode upshifts were different. Kitagawa et al. considered the upshifts as evidence for hydrogen bonding of bound dioxygen to the distal histidine of oxycobalt myoglobin and hemoglobin.[41a] On the other hand, Kincaid et al. observed the vibrational coupling of ν(O−O) and the internal modes of the proximal histidinyl imidazole *trans* to the dioxygen and concluded that the observed upshifts were derived from the changes of the coupling because of an alteration in the internal modes of the imidazole group (which has also an exchangeable proton) due to H/D exchange.[41b,c] In the present case, the possibility of the coupling effect can be ruled out by the following experimental results: (1) The −64 cm^{-1} shift upon ^{18}O substitution matches well the shift of −65 cm^{-1} predicted by Hooke's law for a diatomic O−O stretch. (2) In the structures of both **TCP-TB** and **TCP-TG** complexes, exchangeable protons exist only in the inner hydroxyl groups of the binaphthalene moieties near the iron center, not in the trans axial ligand. We therefore conclude that the bound oxygen in **TCP-TB** and **TCP-TG** interacts with the adjacent exchangeable protons and that the dioxygen adducts of these complexes are stabilized by the hydrogen bonds between the dioxygen and the inner hydroxyl groups, as predicted in the molecular design.

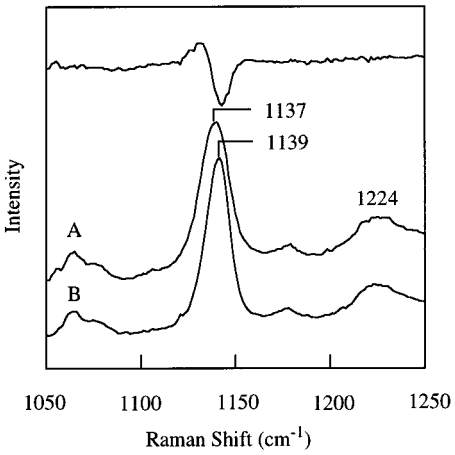

Figure 4. Selected region of resonance Raman spectra of the dioxygen adduct of **TCP-TG** on H/D exchange experiment. THF/CH_3CN, −80 °C, 413.1 nm excitation, 20 mW: trace **A**, CH_3OH; trace **B**, CD_3OD; top, difference spectrum **A** − **B**. The RR spectra of the dioxygen adduct of **TCP-TB** on H/D exchange experiment are included in Supporting Information.

Table 6. Comparison of ν(O−O) Frequencies on H/D Exchange Experiment

complex	ν(O−O)/cm^{-1}		Δ(H/D)/cm^{-1}	ref
$CoMbO_2$	1134 (H_2O)	1136 (D_2O)	2	41a
$CoMbO_2$	1136 (H_2O)	1139 (D_2O)	3	41b
$CoHbO_2$	1133 (H_2O)	1138 (D_2O)	5	41a
$CoHbO_2$	1136 (H_2O)	1140 (D_2O)	4	41b
(**TCP-TB**)Fe−O_2	1138 (CH_3OH)	1140 (CD_3OD)	2	this work
(**TCP-TG**)Fe−O_2	1137 (CH_3OH)	1139 (CD_3OD)	2	this work

Conclusions

Synthesis and characterization of novel iron porphyrins, designated **TCP-TB** and **TCP-TG**, with an alkanethiolate axial

(38) Chottard, G.; Schapracher, M.; Ricard, L.; Weiss, R. *Inorg. Chem.* **1984**, *23*, 4557.
(39) Brunner, H. *Naturwissenschaften* **1974**, *61*, 129.
(40) Tsubaki, M.; Yu, N.-T. *Proc. Natl. Acad. Sci. U.S.A.* **1981**, *78*, 3581.
(41) (a) Kitagawa, T.; Ondrias, M. R.; Rousseau, D. L.; Ikeda-Saito, M.; Yonetani, T. *Nature* **1982**, *298*, 869. (b) Bruha, A.; Kincaid, J. R. *J. Am. Chem. Soc.* **1988**, *110*, 6006. (c) Proniewicz, L. M.; Kincaid, J. R. *Coord. Chem. Rev.* **1997**, *161*, 881.

ligand were carried out to mimic the active center of cytochrome P450. Ferric **TCP-TB** and **TCP-TG** showed sufficient stability for usual manipulation under air and were characterized by means of HR-FAB-MS, UV/vis, ESR, and CV. The corresponding stable dioxygen adducts were obtained by reaction of the ferric complexes with an equimolar amount of KO_2 under an oxygen atmosphere. The frequencies of ν(O−O) bands in the RR spectra were determined to be 1138 cm^{-1} for **TCP-TB** and 1137 cm^{-1} for **TCP-TG**. Finally, direct evidence for hydrogen bonding of the bound dioxygen to the distal hydroxyl groups was obtained also by RR spectroscopy.

It has been long accepted that the hydrogen bonds to bound dioxygen stabilize the oxy-complexes of globins and their nitrogen-base coordinated models.[11,42] In contrast, oxy complexes of thiolate-ligated iron porphyrins are much less stable. However, an analogous hydrogen bond in oxy cytochrome P450 has been very recently revealed by cryocrystallographic techniques.[8] To the best of our knowledge, the present work also shows the first clear evidence for a hydrogen bond to dioxygen in a thiolate-coordinated model. These results have implications in studies of the process of binding and activation of dioxygen by cytochrome P450. These cytochrome P450 model dioxygen adducts could be promising candidates which may lead up to isolation of peroxy-, hydroperoxy-, and high-valent oxo species, which correspond to long-sought, but not-yet-identified, intermediates in the catalytic cycle of cytochrome P450.

Experimental Section

General. All reagents and solvents were of the commercial reagent grade and were used without further purification except where noted. Purification was made by the standard methods.[43] Preparation and handling of air-sensitive materials were carried out under N_2 in a glovebox (M. Braun 150B-G-II or VAC Dri-Lab-08/85) equipped with a circulating purifier (O_2, H_2O < 1 ppm). Dry ether and THF were obtained by predrying over $CaCl_2$ or KOH, and distillation from benzophenone ketyl under N_2 atmosphere. Absolute THF was obtained by redistillation over potassium in a glovebox. Acetonitrile was distilled from P_2O_5 twice and redistilled from K_2CO_3. Then, dry CH_3CN was obtained by redistillation from CaH_2 in a glovebox. Dry THF and dry CH_3CN were treated in the same manner as that described by Selke et al.[44] These solvents were stirred over KO_2 (Aldrich) for ∼1 h and subsequently passed through activated alumina. Activated alumina (Wako) was dried at 220 °C in vacuo for 8 h before use. Deoxygenation of solvents was achieved by a freeze-and-thaw technique under high vacuum conditions (<10^{-5} Torr). $K^{18}O_2$ was prepared according to the literature.[45]

Instruments. ^{1}H NMR spectra were recorded on a JEOL JMX-GX400 (400 MHz) or a Bruker DRX600 (600 MHz) spectrometer. Chemical shifts were reported on *d*-scale relative to tetramethylsilane (TMS). High-resolution mass (HRMS) spectra were recorded on a JEOL LMS-HX-110 spectrometer. FAB-MS spectra were measured with 3-nitrobenzyl alcohol (NBA) or magic bullet as matrices. Electrospray ionization mass (ESI-MS) spectra were obtained on a Perkin-Elmer Sciex API 300 mass spectrometer. Scanning was in 0.1-Da steps and a 10-ms dwell time per step. The orifice voltage was controlled at +60 V. UV/vis electronic spectra were recorded on a Shimadzu UV-3100PC spectrophotometer or a HAMAMATSU PMA-11 CCD spectrophotometer with a Photal MC-2530 as a light source (D_2/W_2). The temperature was controlled by a NESLAB ULT-95 low-temperature circulator. Infrared spectra were recorded on a BIO RAD FTS-6000 spectrometer. ESR spectra were obtained at 77 K in 5.0 mm diameter ESR quartz tubes on a JEOL JES-TE 300 spectrometer. The magnetic field strength was calibrated by the hyperfine coupling constants (hfcc) of Mn(II) ion doped in MgO powder (86.9 G). Redox potentials of **TCP-TB**, **TCP-TG**, and FeTMPCl (0.5 mM) in dried CH_3CN containing 0.1 M tetra-*n*-butylammonium tetrafluoroborate (Bu_4NBF_4) as a supporting electrolyte were determined at room temperature by cyclic voltammetry using a three-electrode system under deaerated conditions and a BAS 100B electrochemical analyzer. Platinum wires were used as working and counter electrodes. The reversibility of the electrochemical processes was evaluated by standard procedures, and all potentials were recorded against an Ag/Ag^+ reference electrode, which was calibrated using the ferrocene/ferrocenium redox couple. Resonance Raman spectra were obtained on a SpectraPro-300i (Acton Research Co.) spectrograph (operating at a 2400-groove grating) using a Spectra-Physics Beamlok 2060 Kr ion laser (413.1 nm) or a KIMMON Electric IK4152R-G He−Cd laser (441.6 nm), a Kaiser Optical holographic supernotch filter, and a Princeton Instruments (LN-1100PB) liquid-N_2-cooled CCD detector. Spectra were collected on solution samples in spinning cells (2-cm diameter, 1500 rpm) with a laser power of 20 mW, 90°-scattering geometry, and 5-min data accumulation. The temperature was monitored with a thermocouple at the sample point and controlled by the flow rate of cold nitrogen gas, which flowed through liquid N_2 to a cell in a quartz Dewar. Peak frequencies were calibrated relative to indene and CCl_4 standards and were accurate to ±1 cm^{-1}. During each Raman experiment, UV/vis spectra were simultaneously collected on a HAMAMATSU PMA-11 CCD spectrophotometer with Photal MC-2530 as a light source (D_2/W_2).

Synthesis of TCP-TB and TCP-TG complexes. 9a and 9b. The octahydroxylated porphyrin **1** (281 mg, 0.38 mmol) and the chloride **5** (688 mg, 1.46 mmol) were separately dried in vacuo (<10^{-6} Torr) overnight. They were introduced into a glovebox and mixed in an autoclave (300 mL) together with K_2CO_3 (2.31 g), dry degassed THF (195 mL) and dry degassed NMP (39 mL). The autoclave was taken out, and heated for 4 days at 115 °C. The chloride **5** (each ∼160 mg) was further added to the mixture subsequently 2 and 4 days later, depending on the progress of the coupling reaction. The aliquot was taken and checked by ESI-MS. After 4 days, THF was evaporated, and the residue was poured into water to afford purple solids, followed by suction filtration. The precipitates were purified by alumina column chromatography (CH_2Cl_2/AcOEt = 9/1, v/v). The crude product was further purified by flash column chromatography (silica gel, CH_2Cl_2/MeOH = 50/1, v/v). The less polar fraction contained the eclipsed isomer **9a** (171 mg, 7.3×10^{-2} mmol, 19%), and the more polar one included the staggered one **9b** (88 mg, 3.8×10^{-2} mmol, 10%). Each of the title compounds, eclipsed and staggered isomers, was obtained as purple solids (total yield 29%).

The eclipsed isomer **9a**: UV/vis (CH_2Cl_2) λ_{max} (10^{-3} ϵ, $M^{-1}\cdot cm^{-1}$) 316 (24.3), 329 (25.7), 407 (57.7), 424 (304), 517 (13.3), 549 (4.59), 591 (5.38), 648 nm (1.97); IR (neat) 3318, 3059, 2933, 2876, 1586, 1453, 1356, 1233, 1204, 1155, 1069, 976, 913, 794, 750, 718 cm^{-1}; HRMS (FAB, NBA, $C_{148}H_{119}N_4O_{24}$) calcd 2335.8214, found 2335.8215.

The staggered isomer **9b**: UV/vis (CH_2Cl_2) λ_{max} (10^{-3} ϵ, $M^{-1}\cdot cm^{-1}$) 329 (34.6), 407 (80.9), 423 (391), 516 (20), 546 (5.5), 591 (7.2), 646 nm (2.1); HRMS (FAB, NBA, $C_{148}H_{119}N_4O_{24}$) calcd 2335.8214, found 2335.8184.

10. The eclipsed isomer **9a** (50 mg, 2.1×10^{-2} mmol) was dried in vacuo for 1−2 h, and then placed under Ar. Dry dichloromethane was added to the flask, and then bromotrimethylsilane (88 mL, 0.68 mmol) was added dropwise at −40 °C. The formation of title compound was monitored by TLC (silica gel, dichloromethane), and the reaction temperature was gradually raised to −20 °C. After 4−5 h later, the reaction mixture was poured into cold saturated aqueous $NaHCO_3$ and extracted with CH_2Cl_2. The combined organic layer was washed with saturated aqueous $NaHCO_3$ and brine and then dried over Na_2SO_4. After evaporation of the solvent, the crude product was dried in vacuo for 1 h and then washed with methanol. Insoluble purple solids were filtered to give the title compound (40 mg, 0.02 mmol, yield 96%). UV/vis (CH_2Cl_2) λ_{max} (10^{-3} ϵ, $M^{-1}\cdot cm^{-1}$) 325 (30), 337 (33.7), 407 (52), 424 (285), 518 (13.5), 550 (3.7), 591 (4.3), 646 nm (1.3); IR (neat) 3458,

(42) Jameson, G. B.; Ibers, J. A. In *Bioinorganic Chemistry*; Bertini, I., Gray, H. B., Lippard, S., Valentine, J., Eds.; University Science Books: California, 1994; pp 167−252.

(43) Perrin, D. D.; Armarego, W. L. F. *Purification of Laboratory Chemicals*, 3rd ed.; Pergamon Press: Oxford, 1988.

(44) Selke, M.; Sisemore, M. F.; Valentine, J. S. *J. Am. Chem. Soc.* **1996**, *118*, 2008.

(45) Brauer, G. Ed. In *Handbook of Preparative Inorganic Chemistry*; Academic Press: New York, 1963; Vol. 1, p 981.

3068, 2959, 2929, 1629, 1595, 1454, 1384, 1369, 1259, 1232, 1111, 1083, 982, 966, 792, 749, 724 cm^{-1}; HRMS (FAB, NBA, $C_{132}H_{87}N_4O_{16}$) calcd 1983.6117, found 1983.6115.

11. The deprotected porphyrin **10** (65 mg, 3.3×10^{-2} mmol) was dried in vacuo for 1 h, and then placed under Ar. Dry CH_2Cl_2 (40 mL) was added to the reaction flask and cooled to 0 °C under N_2, and pyridine (4.0 mL, 50 mmol) was added. Then, pivaloyl chloride (1.3 mL, 10 mmol) was added to the mixture dropwise. After stirring overnight at room temperature, the reaction mixture was cooled again to 0 °C, quenched with 1 N HCl, and then extracted with CH_2Cl_2. The combined organic layer was washed with 1 N HCl, saturated aqueous $NaHCO_3$ (three times), water, and brine and then dried over Na_2SO_4. The crude product was purified by flash column chromatography (silica gel, CH_2Cl_2/EtOH = 200/1, v/v). The title compound **11** was obtained as purple solids (74 mg, 3.2×10^{-2} mmol, yield 97%). UV/vis (CH_2Cl_2) λ_{max} (10^{-3} ϵ, $M^{-1}\cdot cm^{-1}$) 325 (29.7), 338 (28.9), 375 (17.4), 405 (55.1), 423 (308), 517 (15), 547 (5), 588 (6.3), 642 nm (2.4); IR (neat) 3457, 3316, 3061, 2973, 2934, 2874, 1745, 1631, 1585, 1455, 1368, 1261, 1231, 1111, 1083, 1007, 893, 789, 749, 719 cm^{-1}; HRMS (FAB, NBA, $C_{152}H_{119}N_4O_{20}$) calcd 2319.8418, found 2319.8376.

12. The porphyrin **11** (15.8 mg, 6.8×10^{-3} mmol) and 2-(iodomethyl)benzyl thiobenzoate **7** (27.4 mg, 74.3×10^{-3} mmol) was dried in vacuo for 1 h, and then dry K_2CO_3 (20 mg, 145×10^{-3} mmol) and NMP (2 mL) were added into the flask. The reaction mixture was heated at 90 °C for 15 min. Then the solvent was removed by heating under reduced pressure. A portion was checked by TLC. If the reaction was not complete, NMP was added, and the mixture was heated again. The mixture was finally dried in vacuo, and purified by flash column chromatography (silica gel). The title compound **12** was obtained as purple solids (10.8 mg, 4.2×10^{-3} mmol, yield 62%). ^{1}H NMR (400 MHz, $CDCl_3$) 8.73 (d, J = 4.9 Hz, 1H, pyrrole β-H), 8.70 (d, J = 4.4 Hz, 1H, pyrrole β-H), 8.58 (d, J = 4.4 Hz, 1H, pyrrole β-H), 8.57 (d, J = 4.4 Hz, 1H, pyrrole β-H), 8.54 (d, J = 4.4 Hz, 1H, pyrrole β-H), 8.50 (d, J = 4.9 Hz, 1H, pyrrole β-H), 8.16 (d, J = 4.4 Hz, 1H, pyrrole β-H), 8.11 (d, J = 4.9 Hz, 1H, pyrrole β-H), 8.00 (s, 1H), 7.90 (d, J = 7.8 Hz, 1H), 7.83 (s, 1H), 7.81 (d, J = 9.8 Hz, 1H), 7.71 (m, 4H), 7.53 (m, 10H), 7.44 (s, 1H), 7.38−7.13 (m, 12H), 7.08−6.98 (m, 6H), 6.83 (m, 4H), 6.68 (m, 5H), 6.52 (m, 3H), 6.41 (d, J = 8.3 Hz, 1H), 6.31 (d, J = 8.8 Hz, 1H), 6.13 (d, J = 8.3 Hz, 1H), 6.09 (d, J = 8.8 Hz, 1H), 5.80 (t, J = 7.6 Hz, 1H), 5.41 (d, J = 9.8 Hz, 1H), 5.35 (d, J = 9.3 Hz, 1H), 5.25 (m, 3H), 5.12 (m, 2H), 5.03 (s, 1H), 4.85 (m, 3H), 4.71 (m, 3H), 4.59 (s, 1H), 4.21 (d, J = 13.7 Hz, 1H), 4.16 (d, J = 7.8 Hz, 1H), 4.14 (d, J = 13.7 Hz, 1H), 4.02 (t, J = 7.1 Hz, 1H), 3.66 (t, J = 7.6 Hz, 1H), 3.13 (d, J = 7.3 Hz, 1H), 2.74 (d, J = 13.2 Hz, 1H), 2.53 (d, J = 13.7 Hz, 1H), 1.90 (d, J = 13.7 Hz, 1H), 1.39 (d, J = 11.2 Hz, 1H), 1.21 (d, J = 10.7 Hz, 1H), 0.77 (s, 9H, Piv-CH_3), 0.76 (d, J = 13.7 Hz, 1H), 0.74 (s, 9H, Piv-CH_3), 0.28 (s, 9H, Piv-CH_3), 0.17 (s, 9H, Piv-CH_3), −3.62 (s, 2H, NH); UV/vis (CH_2Cl_2): λ_{max} (10^{-3} ϵ, $M^{-1}\cdot cm^{-1}$) 325 (22.7), 406 (25.8), 427 (272) and 553 nm (14.0); IR (neat) 3483, 3310, 3060, 2961, 2929, 2874, 1746, 1585, 1457, 1365, 1260, 1230, 1111, 1082, 892, 791, 748, 718 cm^{-1}; HRMS (FAB, NBA, $C_{167}H_{131}N_4O_{21}S$) calcd 2559.9027, found 2559.9016.

13. The porphyrin **12** (5.3 mg, 2.1×10^{-3} mmol) was dried in vacuo for 2 h. Dry toluene (10 mL) was added to the reaction flask. The mixture was heated in an oil bath at 50 °C, and $Fe(CO)_5$ (100 mL, 7.45×10^{-1} mmol) and a toluene solution (100 mL) of I_2 (6.5 mg, 2.6×10^{-2} mmol) was added. The reaction mixture was stirred for 1 day at 50 °C under N_2 in the dark. An aliquot was taken and checked by TLC (CH_2Cl_2/MeOH = 100/1, v/v) and ESI-MS. The reaction mixture was quenched with water and extracted with CH_2Cl_2. The combined organic layer was washed with 0.5 N HCl and brine and then dried over Na_2SO_4. After evaporation of the solvent, the residue was purified by flash column chromatography (silica gel, CH_2Cl_2/MeOH = 100/1, v/v). The title compound **13** was obtained as brown solids (4.2 mg, 1.6×10^{-3} mmol, yield 78%). UV/vis (CH_2Cl_2) λ_{max} (10^{-3} ϵ, $M^{-1}\cdot cm^{-1}$) 327 (37.1), 423 (77.3), 518 (9.4), 583 (2.7) and 653 (2.0) nm; IR (neat) 3446, 3058, 2965, 2928, 2856, 1745, 1586, 1456, 1367, 1261, 1231, 1110, 1079, 1026, 1003, 895, 797, 750, 720 cm^{-1}; HRMS (FAB, Magic Bullet, $C_{167}H_{128}N_4O_{21}SFe$) calcd 2612.8141, found 2612.8159.

TCP-TB. The iron complex **13** (4.6 mg, 1.8×10^{-3} mmol) was dried in vacuo for 2 h. Dry CH_3CN (2 mL) and dry $BuNH_2$ (0.1 mL, 1 mmol) were added, and the mixture was stirred for 2 days at room temperature in a glovebox. The reaction mixture was quenched with an aqueous solution (5 mL) of *p*-toluenesulfonic acid (500 mg, 2.90 mmol). The flask was taken out from the glovebox and immediately 1 N HCl (2 mL) was added. The mixture was extracted with CH_2Cl_2. The combined organic layer was washed with water until the aqueous layer became neutral and then with brine, and was dried over Na_2SO_4. The crude product was purified by flash column chromatography (silica gel, CH_2Cl_2/MeOH = 300/1, v/v). **TCP-TB** was obtained as brown solids (2.1 mg, 8.4×10^{-4} mmol, yield 48%). UV/vis (CH_2Cl_2) λ_{max} (10^{-3} ϵ, $M^{-1}\cdot cm^{-1}$) 326 (32.8), 338 (31.3), 416 (Soret, 61.8), 515 (9.83) and 657 (2.69) nm; IR (neat) 3501, 3444, 3059, 2963, 2926, 2855, 1743, 1585, 1456, 1366, 1261, 1084, 1026, 871, 766, 749, 709 cm^{-1}; ESR (THF, 77 K) g = 2.334, 2.210, 1.959; HRMS (FAB, NBA, $C_{160}H_{124}N_4O_{20}SFe$) calcd 2508.7879, found 2508.7866; elemental analysis ($C_{160}H_{123}N_4O_{20}SFe\cdot 6H_2O$) calcd C 73.41, H 5.20, N 2.14; found C 73.57, H 5.61, N 2.34.

14. To a CH_2Cl_2 solution (5 mL) of **11** (29.7 mg, 12.8×10^{-3} mmol), 4-(dimethylamino)pyridine (15.6 mg, 0.128 mmol), 1-(3-dimethylaminopropyl)-3-ethylcarbodiimide hydrochloride (22.4 mg, 0.128 mmol), and ethyldisulfanylacetic acid **8** (15.3 mL, 0.128 mmol) were added and stirred at room temperature in the dark. After 1 h, the portion of the solution was taken, washed with 1 N HCl and saturated aqueous $NaHCO_3$, and then extracted with CH_2Cl_2. The formation of the title compound was checked by ESI-MS. Before the formation of the undesired compound, in which the two hydroxyl groups were esterified, the reaction mixture was quenched with 1 N HCl, and then extracted with CH_2Cl_2. The combined organic layer was washed successively with saturated aqueous $NaHCO_3$ and brine and then dried over Na_2SO_4. After evaporation of the solvent, the crude product was purified by flash column chromatography (silica gel, CH_2Cl_2/EtOH). The title compound **14** was obtained as purple solids (11.2 mg, 4.56×10^{-3} mmol, 36%). ^{1}H NMR (400 MHz, $CDCl_3$) 8.82 (d, J = 4.4 Hz, 1H, pyrrole β-H), 8.79 (d, J = 4.9 Hz, 1H, pyrrole β-H), 8.77 (d, J = 4.4 Hz, 1H, pyrrole β-H), 8.76 (d, J = 4.9 Hz, 1H, pyrrole β-H), 8.62 (d, J = 4.9 Hz, 1H, pyrrole β-H), 8.55 (d, J = 4.4 Hz, 1H, pyrrole β-H), 8.30 (d, J = 4.4 Hz, 1H, pyrrole β-H), 8.27 (d, J = 4.9 Hz, 1H, pyrrole β-H), 7.88−6.50 (m, 46H, aromatic-H), 6.43 (d, J = 8.8 Hz, 1H, aromatic-H), 6.34 (d, J = 8.3 Hz, 1H, aromatic-H), 6.10 (d, J = 8.3 Hz, 1H, aromatic-H), 6.08 (d, J = 5.9 Hz, 1H, aromatic-H), 5.87 (m, 2H, aromatic-H), 5.34−4.70 (m, 11H, benzyl-CH_2), 4.34 (d, J = 14.2 Hz, 1H, benzyl-CH_2), 4.22 (d, J = 13.7 Hz, 1H, benzyl-CH_2), 4.21 (d, J = 13.2 Hz, 1H, benzyl-CH_2), 2.66 (d, J = 13.2 Hz, 1H, benzyl-CH_2), 2.52 (d, J = 14.2 Hz, 1H, benzyl-CH_2), 0.73 (s, 9H, Piv-CH_3), 0.68 (s, 9H, Piv-CH_3), 0.33 (s, 9H, Piv-CH_3), 0.23 (s, 9H, Piv-CH_3), −0.44 (m, 1H, S$CH_2$$CH_3$), −0.50 (t, J = 6.8 Hz, 3H, S$CH_2$$CH_3$), −1.20 (m, 1H, S$CH_2$$CH_3$), −2.15 (d, J = 18.6 Hz, 1H, $COCH_2$S), −2.72 (d, J = 18.6 Hz, 1H, $COCH_2$S), −2.94 (s, 2H, NH); UV/vis (CH_2Cl_2) λ_{max} (10^{-3} ϵ, $M^{-1}\cdot cm^{-1}$) 325 (19.1), 338 (18.3), 402 (39), 422 (211.6), 518 (11.8), 587 (4), 640 nm (1.4); IR (neat) 3458, 3333, 3305, 3056, 2958, 2926, 2875, 2853, 1747, 1585, 1457, 1367, 1260, 1231, 1110, 1082, 1025, 796, 748, 719 cm^{-1}; HRMS ($C_{156}H_{125}O_{21}N_4S_2$) calcd 2453.8278, found 2453.8284.

TCP-TG. 14 (5.3 mg, 2.16×10^{-3} mmol) was dissolved in dry toluene (10 mL) and heated at 50 °C under N_2. $Fe(CO)_5$ (105 mL, 0.78 mmol) and a toluene solution of I_2 (6.8 mg, 26.8×10^{-3} mmol) were added. The mixture was stirred overnight in the dark, quenched with water, and then extracted with CH_2Cl_2. After removal of the solvent and drying, the residue was purified by flash column chromatography (silica gel, CH_2Cl_2). **TCP-TG** was obtained as brown solids (3.6 mg, 1.47×10^{-3} mmol, 41%) and the thiolate-protected complex **15** was also obtained as a minor product (1.5 mg, 0.59×10^{-3} mmol, 16%). **TCP-TG**: UV/vis (CH_2Cl_2) λ_{max} (10^{-3} ϵ, $M^{-1}\cdot cm^{-1}$) 325 (18.2), 339 (18.7), 363 (17.1), 418 (31.6), 513 (5.8), 575 (2.7), 658 nm (1.7); IR (neat) 3453, 3062, 2957, 2927, 2873, 1746, 1585, 1456, 1367, 1260, 1229, 1111, 1085, 997, 788, 747, 719 cm^{-1}; ESR (THF, 77 K) g = 2.313, 2.209, 1.966; HRMS ($C_{154}H_{118}O_{21}N_4SFe$) calcd 2446.7359, found 2446.7417; elemental analysis ($C_{154}H_{117}O_{21}N_4SFe\cdot 8H_2O$) calcd C 71.37, H 5.17, N 2.16; found C 71.66, H 5.49, N 1.94. **15**: UV/vis (CH_2Cl_2) λ_{max} (10^{-3} ϵ, $M^{-1}\cdot cm^{-1}$) 325 (19.1), 338 (18.3), 402 (39), 422 (211.6), 518 (11.8), 587 (4) and 640 (1.4) nm; IR (neat) 3474, 3057, 2960,

2928, 2874, 1747, 1586, 1456, 1365, 1261, 1232, 1110, 1085, 999, 890, 794, 748, 717 cm^{-1}; HRMS (FAB, NBA, $C_{156}H_{123}N_4O_{21}S_2Fe$) calcd 2507.7471, found 2507.7478.

Reaction of TCP-TB and TCP-TG with KO_2. TCP-TB, or **TCP-TG** (0.2 mg, 8.2×10^{-5} mmol) was dissolved in THF (0.6 mL, 1.37×10^{-4} M) in a glovebox. The solution was cooled to −80 °C, and then a solution of KO_2 (50 μL, CH_3CN, 1.65×10^{-3} M), which was dissolved with cryptand [2.2.2], was added into the porphyrin solution. After the replacement of the atmosphere to O_2, the resulting solution was subjected to UV/vis absorption and resonance Raman spectroscopy.

Acknowledgment. This research was financially supported by Grant-in-Aids for COE Research (No. 08CE2005 to Y.N.), for Scientific Research on Priority Areas (No. 09235225 and 11228207 to Y.N.), and for Encouragement of Young Scientists (No. 08740500 to F.T.) from the Ministry of Education, Science and Culture, Japan and by Research Grants to Y.N. from Sumitomo Foundation and to F.T. from Takeda Science Foundation and Otsuka Chemical Co. Ltd.

Supporting Information Available: Experimental details relative to the syntheses and characterization of the binaphthyl derivatives (**2**−**5**), the porphyrin compounds and the protected thiolate compounds (**6**−**8**), ^1H NMR data of **9a**−**11**, and RR spectra of the dioxygen adduct of **TCP-TB** (PDF). This material is available free of charge via the Internet at http://pubs.acs.org.

JA003430Y